DØ Note 5695-CONF
Version 1.3

Search for charged Higgs bosons decaying to top and bottom quarks in $p\bar{p}$ collisions

The DØ Collaboration
URL http://www-d0.fnal.gov
(Dated: July 5, 2008)

We describe a search for production of a charged Higgs boson, $q\bar{q}' \to H^+$, reconstructed in the $t\bar{b}$ final state in the mass range $180 \leq M_{H^+} \leq 300$ GeV. The search was undertaken at the Fermilab Tevatron collider with a center-of-mass energy $\sqrt{s} = 1.96$ TeV and uses 0.9 fb^{-1} of data collected with the D0 detector. We find no evidence for charged Higgs boson production and set upper limits on the production cross section in the Types I, II and III two-Higgs-doublet models (2HDMs). An excluded region in the $(M_{H^+}, \tan\beta)$ plane for Type I 2HDM is presented.

Preliminary Results for Summer 2008 Conferences

In the standard model (SM), one $SU(2)$ doublet induces electroweak symmetry breaking, which leads to a single elementary scalar particle: the neutral Higgs boson. Two $SU(2)$ doublets perform the task of electroweak symmetry breaking in two-Higgs-doublet models (2HDMs) [1]. This leads to five physical Higgs bosons among which two carry charge. Hence the discovery of a charged Higgs boson would be unambiguous evidence of new physics beyond the SM. Various types of 2HDMs are distinguished by their strategy for avoiding flavor-changing neutral currents (FCNCs). In the Type I 2HDM, only one of these doublets couples to fermions. In the Type II 2HDM, a symmetry is imposed so that one doublet couples to up-type fermions and the other couples to down-type fermions; an approach used in minimal supersymmetry extensions [1]. In Type III 2HDMs, both doublets couple to fermions, no symmetry is imposed and FCNCs are avoided by other methods. For example, in one Type III model, FCNCs are suppressed by the small mass of the first and second generation quarks [2].

In this Letter we present the first search for a charged Higgs boson (H^+) directly produced by quark-antiquark annihilation, and decaying into the $t\bar{b}$ [3] final state, in the $180 \leq M_{H^+} \leq 300$ GeV mass range. In most models this decay dominates for large regions of parameter space when the H^+ mass (M_{H^+}) is greater than the mass of the top quark (m_t). Exploring the mass range $M_{H^+} > m_t$ is complementary to previous Tevatron searches [4] that have been performed in top quark decays for the $M_{H^+} < m_t$ region. We analyze 0.9 fb^{-1} of data from $p\bar{p}$ collisions at a center-of-mass energy of $\sqrt{s} = 1.96$ TeV recorded from August 2002 to December 2006 using the D0 detector [5]. Since the D0 single top quark analysis [6] reconstructs precisely the same final state in the s-channel $W^+ \to t\bar{b}$ process, we use the dataset from that search.

Direct searches for a charged Higgs boson have been performed at the CERN e^+e^- collider (LEP) [7] and the Fermilab Tevatron collider [4], while indirect searches have been undertaken at the B factories [8, 9]. No evidence for H^+ has been found so far. Limits on the charged Higgs mass and the ratio of vacuum expectation values of the two Higgs fields ($\tan\beta$) are typically calculated in the context of the Type II 2HDM [10]. The combined results from the LEP experiments and those from B factories yield $M_{H^+} > 78.6$ GeV [10] and $M_{H^+} > 295$ GeV [8], respectively, at the 95% C.L. and assuming Type II 2HDM.

The charged Higgs Yukawa couplings carry information about new physics beyond the SM and it has been noted that 2HDM couplings in Types I and II 2HDM can be quite large [11]. For a Type III 2HDM, large contributions from heavy quark-antiquark annihilation can be expected if the top-quark/charm-quark mixing parameter (ξ^U_{tc}) is large [2]. In many models, if $M_{H^+} > m_t$, then the branching fraction of the charged Higgs boson to $t\bar{b}$ is of order unity, owing to the mass dependence of the couplings and the large top quark mass.

We use the program CompHEP [12] to simulate charged Higgs boson production and selected decay $q\bar{q}' \to H^+ \to t\bar{b} \to W^+b\bar{b} \to \ell^+\nu b\bar{b}$ where ℓ represents an electron or muon. This is done for seven M_{H^+} values ranging from 180 to 300 GeV. The lower mass value is dictated by the kinematics of the decay $H^+ \to t\bar{b}$ which requires $M_{H^+} > m_t + m_b$, where m_b is the mass of the bottom quark. The upper mass value is chosen based on the fact that, in this mass range, the production cross section decreases by approximately an order of magnitude for any of the models considered. The couplings are set to produce pure chiral state samples that are combined in different proportions to simulate the desired 2HDM type. The size of the interference term proportional to the product of the left and right-handed couplings is considered negligible. The size of this interference term is of order 1% of the total amplitude in the $\tan\beta < 30$ region for the Type II 2HDM, much less than 1% for the Type I 2HDM and non-relevant for a Type III 2HDM. Each choice of couplings determines the total width, Γ_{H^+}, and the initial-state quark flavor composition. This quark flavor composition of the signal samples is determined by the value of the element $|V_{ij}|$ of the Cabibbo-Kobayashi-Maskawa (CKM) matrix [13] and the CTEQ6L1 parton distribution functions (PDFs) [16]. In these simulated signal samples, Γ_{H^+} ranges from approximately 4 GeV for $M_{H^+} = 180$ GeV to 9 GeV for $M_{H^+} = 300$ GeV.

In order to simulate the kinematic distributions of a particular model, the left-handed and right-handed signal samples are combined with event weights equal to the fraction of the production cross section associated with the left-handed or right-handed coupling contribution. The Type II 2HDM couplings for right-handed (R) and left-handed (L) chiral states are $V^{qq'}_{CKM} g m_{q'} \tan\beta/(\sqrt{2}M_W)$ and $V^{qq'}_{CKM} g m_q \cot\beta/(\sqrt{2}M_W)$, where $V^{qq'}_{CKM}$ is the CKM matrix element, $m_q/m_{q'}$ the up/down-type quark mass, M_W the mass of the W boson and g the SM weak coupling constant. The $R(L)$ couplings in Type I and III 2HDMs are $V_{qq'} g m_{q'} \tan\beta/(\sqrt{2}M_W)$ ($-V_{qq'} g m_q \tan\beta/(\sqrt{2}M_W)$) and $-(V_{\rm CKM}\hat{Y}_D)_{qq'}$ ($(\hat{Y}^\dagger_U V_{\rm CKM})_{qq'}$), where $\hat{Y}^{U,D}_{ij} = \xi\sqrt{2m_i m_j}/v$, v is the vaccum expectation value and ξ is taken as a free parameter of the model. For the simulation of Type I 2HDM, left-handed and right-handed samples are added in equal proportion. For the simulation of Type II 2HDM, signal samples are combined to simulate four $\tan\beta$ values or ranges: $\tan\beta < 0.1$, $\tan\beta = 1$, $\tan\beta = 5$, and $\tan\beta > 10$. The Type I 2HDM and $\tan\beta = 1$ Type II models share the same left/right-handed proportions. For the Type III 2HDM as described in [2], quark-antiquark annihilation is dominated by right-handed couplings. This model is simulated using the same proportions of left-handed and right-handed samples as used to simulate the $\tan\beta > 10$ Type II model. This approach provides an adequate simulation of signal event kinematics only for model parameter values that result in a charged Higgs width comparable or smaller than the experimental mass resolution of $\mathcal{O}(10)$ GeV.

Background contributions from W+jets and top quark pair ($t\bar{t}$) production are modeled using the ALPGEN Monte

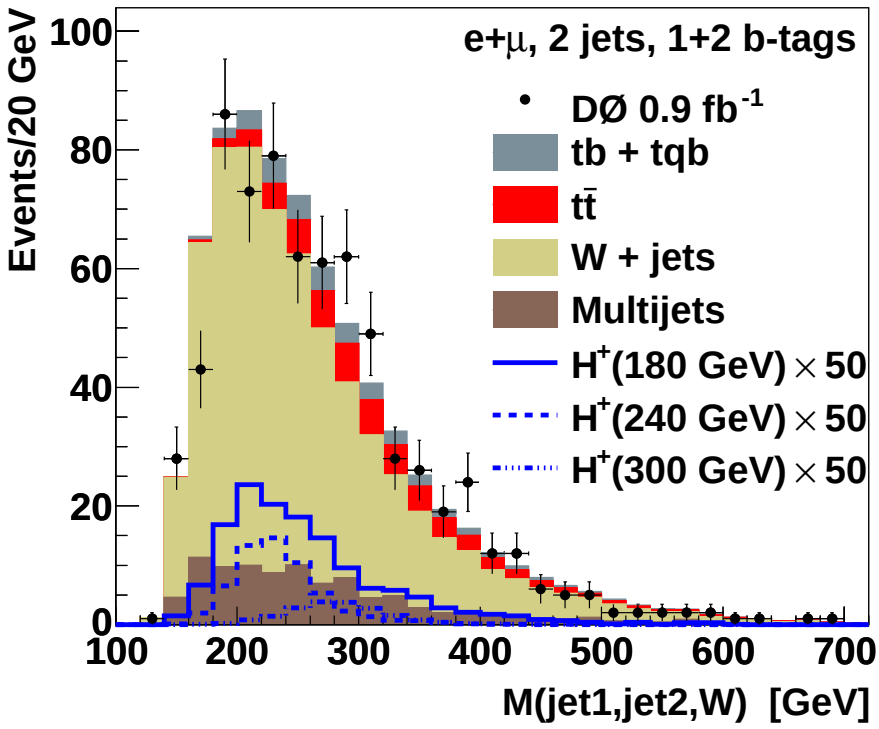

FIG. 1: Distribution of the discriminating variable, $M(\text{jet1}, \text{jet2}, W)$, for the signal, background model and data, for the combined electron and muon channels with exactly two jets and with one or two b tags. The signal distributions correspond to a Type III 2HDM for charged Higgs boson masses $180, 240, 300$ GeV, and are normalized according to the production cross section presented in Ref. [2] scaled by a factor of 50.

Carlo (MC) event generator [14]. The single top quark samples are generated with the SingleTop [15] MC event generator. For both samples, we assume a top quark mass of 175 GeV and use the CTEQ6L1 PDFs. After generation, the events are passed through a GEANT-based simulation [17] of the D0 detector and subsequently through standard reconstruction procedures that correct differences between the simulation and data.

The background contribution from misreconstructed multijet events is modeled using data events containing misidentified leptons and is normalized to the signal data together with the W+jets sample, which contains leptons from the W boson decay [6].

We search for charged Higgs bosons in the $H^+ \to t\bar{b} \to \ell^+\nu b\bar{b}$ final state, and hence require that events satisfy triggers with a jet and an electron or muon. Selections that are identical to the two-jet analysis channel for the D0 single top quark analysis [6] are imposed on each observable in the data, background and charged Higgs boson signal samples to select events with $t\bar{b}$ final state signatures. Events are required to have a primary vertex with three or more tracks attached and a lepton originating from the primary vertex [6]. The electron (muon) channel selection requires only one isolated electron (muon) with $E_T > 15$ ($p_T > 18$) GeV within the pseudorapidity region $|\eta| < 1.1$ (2.0). Events with two isolated leptons are rejected. For both channels, events are required to have missing transverse energy within $15 < \not\!\!E_T < 200$ GeV. We require that events have exactly two jets, with the highest p_T jet satisfying $p_T > 25$ GeV and $|\eta| < 2.5$, and the second jet satisfying $p_T > 20$ GeV and $|\eta| < 3.4$.

Since both jets of the signal events are b jets, we select data events having one or two jets identified as such via a neural network-based tagging algorithm [18]. MC simulated events are weighted using a b-tag probability derived from data. The signal acceptances after the complete selection increase monotonically in the mass range $200 < M_{H^+} < 300$ GeV, for example, from $(0.48 \pm 0.06)\%$ to $(1.24 \pm 0.20)\%$ for $\tan\beta < 0.1$, statistical and systematic uncertainties included. The signal acceptances for a given M_{H^+} decreases by at most 0.12% with increasing $\tan\beta$.

A distinctive feature of signal events is the large mass of the charged Higgs boson. We therefore use the reconstructed invariant mass of the top and bottom quark system as the discriminating variable for the charged Higgs signal. We define this variable as the invariant mass $M(\text{jet1}, \text{jet2}, W)$. In the reconstruction of the W boson, there are up to two possible solutions for the neutrino momentum component along the beam axis (p_z). In these cases, the solution with the smallest absolute value of the p_z momentum is chosen. Figure 1 shows the $M(\text{jet1}, \text{jet2}, W)$ distribution after selection, with an example signal normalized to the production cross section for a Type III 2HDM [2] and for three different mass values.

TABLE I: Observed limits on the production cross section (in pb) times branching fraction $\sigma(q\bar{q}' \to H^+) \times \mathcal{B}(H^+ \to t\bar{b})$. The expected limits are shown in parenthesis for comparison. These limits apply to the Type II 2HDM. The limits obtained for $\tan\beta = 1$ and $\tan\beta > 10$ are also valid for Type I and Type III 2HDMs, respectively. Limits shown in square brackets are only valid for the general production of a charged scalar via a purely left-handed coupling with width smaller than the experimental resolution. These limits are not valid for the production of a charged Higgs boson in Type II 2HDM since the charged Higgs width is expected to be larger than the experimental resolution.

M_{H^+} (GeV)	$\tan\beta < 0.1$	$\tan\beta = 1$	$\tan\beta = 5$	$\tan\beta > 10$
180	12.9 (11.4)	14.3 (12.2)	13.7 (11.7)	13.7 (12.2)
200	[5.9 (9.6)]	6.3 (9.9)	6.5 (10.0)	6.5 (10.0)
220	[2.9 (4.2)]	3.0 (4.4)	3.0 (4.5)	3.0 (4.5)
240	[2.3 (3.1)]	2.4 (3.3)	2.6 (3.5)	2.6 (3.5)
260	[3.0 (2.8)]	3.0 (2.9)	3.0 (3.0)	3.0 (3.0)
280	[4.0 (2.6)]	4.2 (2.7)	4.5 (2.9)	4.5 (2.9)
300	[4.5 (2.4)]	4.7 (2.4)	4.9 (2.5)	4.9 (2.5)

The data yield for all analysis channels combined amounts to 697 events, after the complete selection. Similarly, for the sum of all background sources, the total expected yield is 721±42. For the separate background sources, the yields are 531 for W+jets, 95 for multijets, 59 for $t\bar{t}$ and 36 for the single top background.

The systematic uncertainties on the signal and background model are estimated using the methods described in Ref. [6]. Two of the dominant sources of systematic uncertainty arise from the jet energy scale (JES) correction uncertainty and the uncertainty on the b-tag rates applied to MC events (described above). For the H^+ signal, the uncertainty on the model-dependent proportion of initial-state parton flavor contribution plays a dominant role. Simulated signal events with different exclusive initial-state quark combinations are used to assess the latter source of uncertainty. A value of 10% is assigned based on variations in yield and shape of the reconstructed invariant mass distribution.

We observe no excess of data over background and proceed to set upper limits on H^+ boson production. We construct a binned likelihood function and use Bayesian statistics to calculate upper limits on the signal production cross section times the branching fraction ($\sigma \times \mathcal{B}$) to the $t\bar{b}$ final state. A flat positive prior is used for the signal cross section. All sources of systematic uncertainty and their correlations are taken into account in calculating $\sigma \times \mathcal{B}$ upper limits for different 2HDM types at the 95% C.L. At the level of precision reported, the observed limits are insensitive to changes in top mass in the range $170 < m_t < 175$ GeV. The observed and expected $\sigma \times \mathcal{B}$ limits are reported in Table I.

The $\sigma \times \mathcal{B}$ upper limits obtained are compared to the expected signal cross section in the Type I 2HDM to exclude a region of the M_{H^+} and $\tan\beta$ parameter space, shown in Fig. 2. The analysis sensitivity is currently not sufficient to exclude regions of $\tan\beta < 100$ in the Type II 2HDM. In a Type III 2HDM [2], the charged Higgs boson width depends quadratically on the mixing parameter ξ. This limits our ability to exclude regions in the M_{H^+} and ξ parameter space.

In summary, we have performed the first direct search for the production of charged Higgs bosons in the reaction $q\bar{q}' \to H^+ \to t\bar{b}$ and we have presented limits on the production cross section times branching fraction for Types I, II and III 2HDMs in the mass range $180 \leq M_{H^+} \leq 300$ GeV. A region in the M_{H^+} vs $\tan\beta$ plane has been excluded at the 95% C.L. for Type I 2HDMs.

We thank the staffs at Fermilab and collaborating institutions, and acknowledge support from the DOE and NSF (USA); CEA and CNRS/IN2P3 (France); FASI, Rosatom and RFBR (Russia); CNPq, FAPERJ, FAPESP and FUNDUNESP (Brazil); DAE and DST (India); Colciencias (Colombia); CONACyT (Mexico); KRF and KOSEF (Korea); CONICET and UBACyT (Argentina); FOM (The Netherlands); STFC (United Kingdom); MSMT and GACR (Czech Republic); CRC Program, CFI, NSERC and WestGrid Project (Canada); BMBF and DFG (Germany); SFI (Ireland); The Swedish Research Council (Sweden); CAS and CNSF (China); and the Alexander von Humboldt Foundation (Germany).

[a] Visitor from Augustana College, Sioux Falls, SD, USA.
[b] Visitor from The University of Liverpool, Liverpool, UK.
[c] Visitor from ICN-UNAM, Mexico City, Mexico.
[d] Visitor from II. Physikalisches Institut, Georg-August-University, Göttingen, Germany.
[e] Visitor from Helsinki Institute of Physics, Helsinki, Finland.

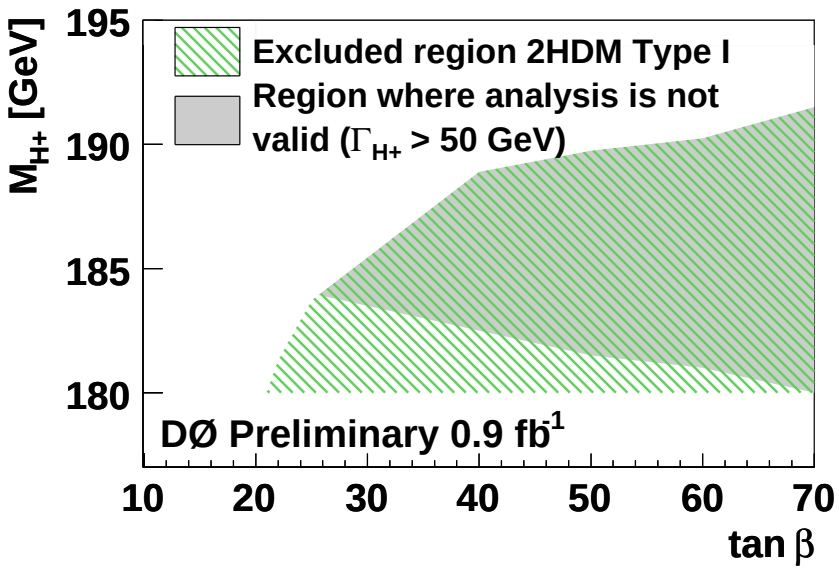

FIG. 2: The 95% C.L. excluded region in the M_{H^+} vs $\tan\beta$ space for Type I 2HDM. The region for which $\Gamma_{H^+} > 50$ GeV indicates the approximate area where the charged Higgs width is significantly larger than the detector resolution and hence the analysis is not valid.

[f] Visitor from Universität Zürich, Zürich, Switzerland.
[‡] Deceased.

[1] J. Gunion *et al.*, *The Higgs Hunter's Guide*, Frontiers in Physics (Addison-Wesley, Redwood City, CA, 1990).
[2] H.-J. He and C.-P. Yuan, Phys. Rev. Lett. **83**, 28 (1999).
[3] We use the H^+ notation to refer to both H^+ and its charge conjugate state H^-. Similarly, the $t\bar{b}$ notation is used here to represent both the $t\bar{b}$ state and its charge conjugate state $\bar{t}b$.
[4] B. Abbott *et al.* (D0 Collaboration), Phys. Rev. Lett. **82**, 4975 (1999); V.M. Abazov *et al.* (D0 Collaboration), Phys. Rev. Lett. **88**, 151803 (2002); A. Abulencia *et al.* (CDF Collaboration), Phys. Rev. Lett. **96**, 042003 (2006).
[5] V.M. Abazov *et al.* (D0 Collaboration), Nucl. Instrum. Methods A **565**, 463 (2006).
[6] V.M. Abazov *et al.* (D0 Collaboration), Phys. Rev. Lett. **98**, 181802 (2007); V.M. Abazov *et al.* (D0 Collaboration), accepted by Phys. Rev. D, arXiv:0803.0739 [hep-ex].
[7] G. Abbiendi *et al.* (OPAL Collaboration), Eur. Phys. J. C **7**, 407 (1999); R. Barate *et al.* (ALEPH Collaboration), Phys. Lett. B **543**, 1 (2002); J. Abdallah *et al.* (DELPHI Collaboration), Phys. Lett. B **525**, 17 (2002); P. Achard *et al.* (L3 Collaboration), Phys. Lett. B **575**, 208 (2003).
[8] M. Misiak *et al.*, Phys. Rev. Lett. **98**, 022002 (2007).
[9] A.G. Akeroyd and S. Recksiegel, J. Phys. G **29**, 2311 (2003).
[10] W.-M. Yao *et al.*, J. Phys. G **33**, 1 (2006).
[11] D.P. Roy, Mod. Phys. Lett. A **19**, 1813 (2004).
[12] E. Boos *et al.*, (compHEP Collaboration), Nucl. Instrum. Methods A **534**, 250 (2004).
[13] N. Cabibbo, Phys. Rev. Lett. **10**, 531 (1963); M. Kobayashi and K. Maskawa, Prog. Theor. Phys. **49**, 652 (1973).
[14] M.L. Mangano *et al.*, J. High Energy Phys. **0307**, 001 (2003). We used ALPGEN version 2.05.
[15] E. Boos *et al.*, Phys. Atom. Nucl. **69**, 1317 (2006).
[16] J. Pumplin *et al.*, J. High Energy Phys. **0207**, 012 (2002).
[17] R. Brun and F. Carminati, CERN Program Library Long Writeup W5013, 1993.
[18] T. Scanlon, Ph.D. thesis, University of London, 2006.